

Chiral anomaly induced oscillations in the Josephson current in Weyl semimetals

Salah Uddin², Wenye Duan³, Jun Wang⁴, Zhongshui Ma^{3,5}, and Jun-Feng Liu^{1,2*}

¹*Department of Physics, School of Physics and Electronic Engineering,
Guangzhou University, Guangzhou 510006, China*

²*Department of Physics, Southern University of Science and Technology, Shenzhen 518055, China*

³*School of Physics, Peking University, Beijing 100871, China*

⁴*Department of Physics, Southeast University, Nanjing 210096, China and*

⁵*Collaborative Innovation Center of Quantum Matter, Beijing, 100871, China*

Weyl semimetals are a three dimensional topological phase of matter with linearly dispersed Weyl points which appear in pairs and carry opposite chirality. The separation of paired Weyl points allows charge transfer between them in the presence of parallel electric and magnetic fields, which is known as the chiral anomaly. In this paper, we theoretically study the influence of the chiral anomaly induced chiral charge imbalance on the Josephson current in a Weyl superconductor-Weyl semimetal-Weyl superconductor junction. In Weyl superconductors, two types of pairings are considered, namely, zero momentum BCS-like pairing and finite momentum FFLO-like pairing. For BCS-like pairing, we find that the Josephson current exhibits $0-\pi$ transitions and oscillates as a function of $\lambda_0 L$, where λ_0 is the chirality imbalance induced by the parallel electric and magnetic fields and L is the length of the Weyl semimetal. The amplitude of the Josephson current also depends on the angle β between the line connecting two paired Weyl points and the transport direction along the junction. For FFLO-like pairing, the chirality imbalance induced periodic oscillations are absent and the Josephson current is also independent of the angle β . These findings are useful in detecting the chiral anomaly and distinguishing the superconducting pairing mechanism of Weyl semimetals.

I. INTRODUCTION

In the past decade or so, a great progress in condensed matter physics has been made by the discovery of topological insulators^{1,2}. Topological insulators have a bulk energy gap and gapless surface states, which are protected by the time-reversal symmetry. Recently, the topological matter is further extended to Weyl semimetals (WSMs)³. WSM is a three-dimensional (3D) phase where linearly dispersed Weyl cones appear in pairs in momentum space carrying opposite chirality. The separation of Weyl points (WPs) with opposite chirality allows charge transfer between them in the presence of parallel electric and magnetic fields, as a consequence of chiral anomaly^{4,5}. The chiral anomaly is a peculiar non-conservation of chiral charge and is mostly discussed in the context of high-energy physics. In WSMs, the charge density at a single WP is not conserved; the application of parallel \mathbf{E} and \mathbf{B} fields drives charges from one WP to the other with opposite chirality. This charge pumping effect induces a chemical potential difference between two paired WPs, which is also referred to as chiral charge imbalance or chirality imbalance. The chiral anomaly results in unusual transport properties⁶⁻⁸ in WSMs, which have attracted much attention⁹⁻¹⁸.

The WSM phase requires broken time reversal^{19,20} or inversion symmetry^{21,22}. Theoretically, WSM has been predicted from the first principle calculation and successfully observed experimentally in non-centrosymmetric transition metal monophosphides, such as NbP, NbAs, TaP and TaAs²³⁻²⁹. Recent studies show that WSM can also be realized in some other materials, including pyrochlore iridates $A_2Ir_2O_7$ where A is Lanthanide or yttrium element³, the ferromagnetic com-

pound $HgCr_2Se_4$ ³⁰⁻³², multilayer structure made of topological and non-topological insulator thin films²⁰, and magnetically doped Bi_2Se_3 ³³.

The unique physics of WSMs also motivates further research on the superconducting pairing mechanism. Particularly, doped WSMs facilitate two types of superconducting pairings—internode and intra-node pairings. The internode pairing forms zero momentum Bardeen-Schrieffer-Cooper (BCS) state³⁴, while the intra-node pairing exhibits a finite momentum Fulde-Ferrell-Larkin-Ovchinnikov (FFLO) state³⁴⁻³⁶. Different analysis methods yield different energetically preferred pairing states. Mean-field calculations show that FFLO-like pairing is favored for pairing states with even parity (singlet pairing)³⁴. For pairing states with odd parity (triplet pairing), a short and long-range interaction results in FFLO- and BCS-like pairing states as ground states, respectively³⁷. The BCS-like pairing is also predicted to be energetically preferred in the weak coupling regime³⁸. Considering the theoretical controversy on the pairing mechanism in WSMs, the experimental verification is very desirable.

The Josephson effect is one of the powerful tools to identify the superconducting pairing. Recently, the Andreev reflection^{39,40} and Josephson effect⁴¹⁻⁴⁶ in a WSM have been theoretically investigated in several works. It has been predicted that at the interface between a time-reversal breaking WSM and a conventional s-wave superconductor, the singlet pairing requires the intra-node Andreev reflection due to the spin-momentum locking of Weyl fermions⁴²⁻⁴⁴. This extra momentum of the pair gives rise to an unusual oscillation in the Josephson current whose period is proportional to the distance between two paired WPs in momentum space. The effect of quan-

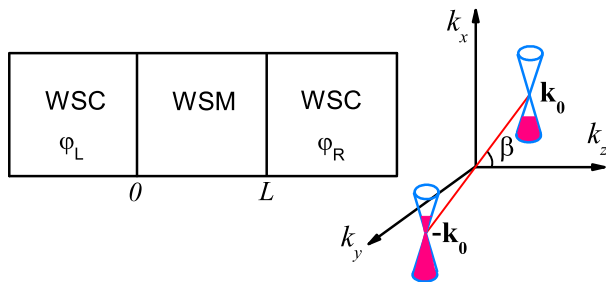


FIG. 1. (Left) Schematic diagram of the WSC-WSM-WSC Josephson junction: A WSM at $0 < z < L$ sandwiched between two WSCs at $z < 0$ and $z > L$. The left (right) WSC is characterized by the phase φ_L (φ_R). (Right) Schematic of the momentum space with two WPs located at $\pm \mathbf{k}_0$ in the k_x - k_z plane, the angle between the line joining the two WPs and the k_z -axis is β . There exists a chirality imbalance between two WPs.

tum interference between the bulk channel and the surface channel in Dirac semimetal based Josephson junction has also been studied recently⁴⁵. However, the investigation in the effect of chiral anomaly on the transport in superconducting heterojunctions is still rare.

In this work, we investigate the Josephson current in a Weyl superconductor (WSC)-WSM-WSC junction as shown in Fig. 1. We consider both BCS- and FFLO-like pairings in two WSCs. For BCS-like pairing, the Josephson current exhibits 0 - π transitions and oscillations that depend on the length of the WSM and the chirality imbalance induced by an $\mathbf{E} \cdot \mathbf{B}$ field. The Josephson current also depends on the angle β between the line connecting two WPs and the transport direction along the junction. For FFLO-like pairing the 0 - π transitions and oscillations are absent and the Josephson current is also independent of β . These findings are useful in detecting the chiral anomaly and distinguishing the superconducting pairing mechanism of Weyl semimetals.

The rest of the paper is organized as follows. In Sec. II, we introduce the model and solve the scattering problem for quasiparticles based on the Bogoliubov-de Gennes (BdG) equation. The Andreev bound states (ABSs) are obtained from the scattering matrices and the Josephson current is obtained from ABSs. In Sec. III, we present the numerical results of Josephson current and Andreev bound states for both BSC- and FFLO-like pairing and discuss the underlying physics. Finally, the conclusion remarks are given in Sec. IV.

II. MODEL AND FORMALISM

The Josephson junction under consideration is sketched in Fig. 1 with two WSCs at $z < 0$ and $z > L$ and a WSM layer in the region $0 < z < L$. The two WPs with opposite chirality are located at $\pm \mathbf{k}_0$ in the k_x - k_z plane, and the line joining two WPs makes an angle β

with the k_z -axis. For such a configuration, an effective two band Hamiltonian for a single WP is used in the references^{39,41}. We use the same model for our present study. The effective two band Hamiltonian around the Weyl node $\pm \mathbf{k}_0$ is

$$H_{\pm} = \hbar\nu(k_1\sigma_1 + k_2\sigma_2 \mp k_3\sigma_3) - \mu_{\pm}, \quad (1)$$

where $\mu_{\pm} = \mu \mp \lambda/2$ is the chemical potential, λ is the chirality imbalance induced by an $\mathbf{E} \cdot \mathbf{B}$ field. And

$$\begin{aligned} k_1 &= k_x \cos \beta - k_z \sin \beta, \\ k_2 &= k_y, \\ k_3 &= k_x \sin \beta + k_z \cos \beta. \end{aligned} \quad (2)$$

Similarly

$$\begin{aligned} \sigma_1 &= \sigma_x \cos \beta - \sigma_z \sin \beta, \\ \sigma_2 &= \sigma_y, \\ \sigma_3 &= \sigma_x \sin \beta + \sigma_z \cos \beta, \end{aligned} \quad (3)$$

where σ_x , σ_y and σ_z are the Pauli matrices. The transport direction is assumed to be along the z -axis. We consider two types of pairing mechanism³⁴. One is the inter-node BCS-like pairing for which two paired electrons are from two different WPs and the Cooper pairs have zero net momentum. The other is the intra-node FFLO-like pairing for which two paired electrons are from one single WP, and the Cooper pairs have nonzero net momentum. In the Nambu representation with four-component bases $[\psi_{\uparrow}(\mathbf{r}), \psi_{\downarrow}(\mathbf{r}), \psi_{\uparrow}^{\dagger}(\mathbf{r}), -\psi_{\downarrow}^{\dagger}(\mathbf{r})]^T$, the BdG Hamiltonians for both BCS- and FFLO-like pairing cases are given by

$$\begin{aligned} H_B^{\pm} &= \begin{pmatrix} H_{\pm}(-i\nabla \mp \mathbf{k}_0) & \Delta(z) \\ \Delta(z)^* & -H_{\mp}(-i\nabla \mp \mathbf{k}_0) \end{pmatrix}, \\ H_F^{\pm} &= \begin{pmatrix} H_{\pm}(-i\nabla \mp \mathbf{k}_0) & \Delta(z)e^{\pm 2i\mathbf{k}_0 \cdot \mathbf{r}} \\ \Delta(z)^*e^{\mp 2i\mathbf{k}_0 \cdot \mathbf{r}} & -H_{\pm}(-i\nabla \pm \mathbf{k}_0) \end{pmatrix}, \end{aligned} \quad (4)$$

where the subscripts B and F correspond to BCS- and FFLO-like pairing respectively. And $\Delta(z) = \Delta_0 [\Theta(-z)e^{i\varphi/2} + \Theta(z-L)e^{-i\varphi/2}]$ denotes the pair potential with Δ_0 as the bulk superconducting gap and $\varphi = \varphi_L - \varphi_R$ as the macroscopic phase difference between the left and right superconductors. The temperature dependence magnitude of Δ is given by $\Delta(T) = \Delta(0) \tanh(1.74\sqrt{T/T_c - 1})$, where T_c is the critical temperature. The chirality imbalance λ is only introduced in the normal WSM region, therefore, $\lambda(z) = \lambda_0 [\Theta(z) - \Theta(z-L)]$. The effective gap for FFLO-like pairing is just $\Delta_F = \Delta_0$, while the effective gap for BCS-like pairing is $\Delta_B = \Delta_0 |\sin \beta|$, which depends on the angle β .

At first, we perform a gauge transformation to remove the large momentum \mathbf{k}_0 from the BdG equation⁴¹. The transformations for BCS-like pairing and FFLO-like pairing are

$$\begin{aligned} H_B^\pm &\longrightarrow \tilde{H}_B^\pm = e^{\pm i\mathbf{k}_0 \cdot \mathbf{r}} H_B^\pm e^{\mp i\mathbf{k}_0 \cdot \mathbf{r}}, \\ H_F^\pm &\longrightarrow \tilde{H}_F^\pm = e^{\pm i\sigma_z \mathbf{k}_0 \cdot \mathbf{r}} H_F^\pm e^{\mp i\sigma_z \mathbf{k}_0 \cdot \mathbf{r}}, \end{aligned} \quad (5)$$

respectively, which gives

$$\begin{aligned} \tilde{H}_B^\pm &= \begin{pmatrix} H_\pm(-i\nabla) & \Delta(z) \\ \Delta(z)^* & -H_\mp(-i\nabla) \end{pmatrix}, \\ \tilde{H}_F^\pm &= \begin{pmatrix} H_\pm(-i\nabla) & \Delta(z) \\ \Delta(z)^* & -H_\pm(-i\nabla) \end{pmatrix}. \end{aligned} \quad (6)$$

Then, the scattering problem of such a junction can be solved by considering the boundary conditions of the wave function at $z = 0$ and $z = L$ ⁴⁷. At each interface we get a scattering matrix, from which the reflection matrix of the right-going (left going) incident particles R_1 (R_2) can be abstracted in the WSM layer. The multiple reflections between the WSM-WSC boundaries lead to bound state levels in the middle WSM layer. The discrete spectrum of these ABSs along a fixed incident direction can be determined by using the condition

$$\det[I_{2 \times 2} - R_2 P R_1 P] |_{E=E_b} = 0, \quad (7)$$

where P is the propagating matrix which accounts for the phases acquired by the electron and hole while moving from one boundary to the other inside the WSM region. In the short junction limit, the Josephson current is mainly carried by the ABSs and can be estimated as

$$I(\varphi) = \frac{2e}{\hbar} \sum_b \frac{\partial E_b}{\partial \varphi} f(E_b), \quad (8)$$

where $f(E_b)$ is the Fermi-Dirac distribution function. The total Josephson current can be obtained as

$$J(\varphi) = \frac{W^2}{(2\pi)^2} \int I(\varphi) dk_x dk_y, \quad (9)$$

where W is assumed to be the dimension in both x and y directions.

III. RESULTS AND DISCUSSIONS

Next we present the numerical results and discussion of the Josephson current in the junction. For simplicity, we introduce the dimensionless units: the wave vector $k \rightarrow k k_0$, the length $L \rightarrow L/k_0$, and the energy $E \rightarrow E E_0$ with $E_0 = \hbar v k_0$. All physical quantities are expressed in these units in the rest of the paper. The superconductors considered are characterized with $\Delta_0 = 10^{-3}$ (in units of E_0) which correspond to the BCS coherence length at zero temperature $\xi_0 = 2/\pi \Delta_0 \approx 636.6$.

First, we consider the effect of λ_0 on the band structure of BCS-like pairing. Fig 2(a) shows the energy dispersion of the WSM for BCS-like pairing, with (red lines) and

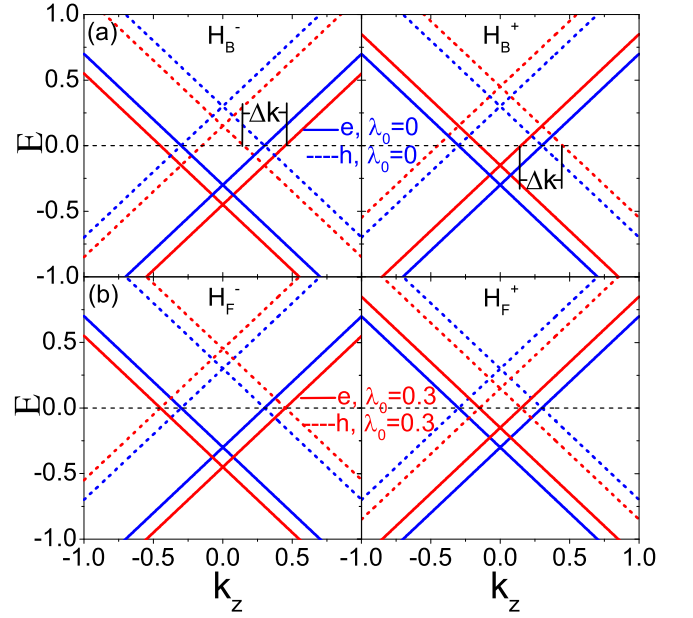


FIG. 2. Energy dispersion $E(k_z)$ of the middle WSM region: (a) for BCS-like pairing and (b) for FFLO-like pairing with $\mu = 0.3$. Solid (dashed) lines are for electrons (holes). Red (Blue) lines are for with (without) the chirality imbalance.

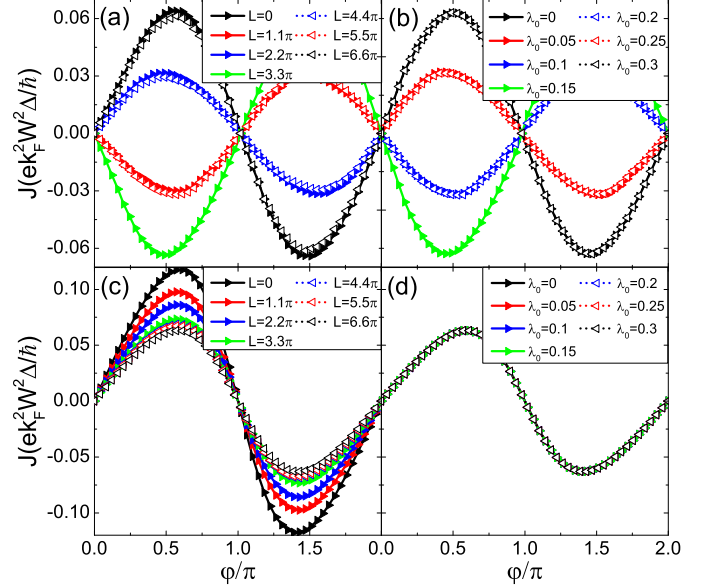


FIG. 3. Josephson current as a function of the superconducting phase difference φ . (a) and (b) are for BCS-like pairing, and (c) and (d) are for FFLO-like pairing. (a) and (c) are for different values of the length L with fixed $\lambda_0 = 0.3$ and (b) and (d) are for different values of λ_0 with fixed $L = 6.6\pi$. The other parameters are $\beta = \pi/4$, $\mu = 0.3$ and $T = 0.5T_c$.

without (blue lines) λ_0 . For a given energy, the wave vectors of propagating electrons and holes are

$$\begin{aligned} k_e^\pm &= \sqrt{\left[\mu \mp \frac{\lambda_0}{2} + E\right]^2 - k_x^2 - k_y^2}, \\ k_h^\pm &= \sqrt{\left[\mu \pm \frac{\lambda_0}{2} - E\right]^2 - k_x^2 - k_y^2}, \end{aligned} \quad (10)$$

where k_e^\pm (k_h^\pm) are wave-vectors of the right going electrons (left going holes) for the pairs H_B^\pm respectively. For normal incidence ($k_x = k_y = 0$), the wave vector difference between the right going electrons and left going holes for the pairs H_B^\pm are $\Delta k^\pm = k_e^\pm - k_h^\pm = \mp \lambda_0$ when $E = 0$. In the formation of Andreev bound states these difference in wave-vectors lead to an additional phase accumulation $\Delta k^\pm L$ due to the traveling of the electron and hole in the WSM layer. These additional phases should be offset by the phase difference between the two superconductors φ . Therefore, the current-phase relations (CPR) for the pairs H_B^\pm have phase shifts $\pm\varphi_0 = \pm\lambda_0 L$. In the first harmonic approximation, the total Josephson current as the summation over two pairs H_B^\pm can be written as

$$\begin{aligned} J &= J_{H_B^+} + J_{H_B^-} \\ &= J_0 \sin(\varphi + \lambda_0 L) + J_0 \sin(\varphi - \lambda_0 L) \\ &= 2J_0 \sin \varphi \cos(\lambda_0 L), \end{aligned} \quad (11)$$

where the critical current $2J_0 \cos(\lambda_0 L)$ implies $0-\pi$ transitions and would change signs with increasing $\lambda_0 L$. This analytical expression of the total Josephson current gives a good fitting of our numerical results (using Eq. (9)) shown in Fig. 3(a) and (b). Fig. 3(a) shows the CPR for different length L of the WSM with fixed $\lambda_0 = 0.3$, and Fig. 3(b) shows the CPR for different λ_0 with fixed $L = 6.6\pi$. The $0-\pi$ transitions are clearly exhibited in Fig. 3(a) and (b) by increasing L or λ_0 .

The energy dispersion of the WSM region for the case of FFLO-like pairing is shown in Fig. 2(b). The paired electrons in FFLO-like pairing are from the same WP, therefore, the wave-vectors difference induced by the chirality imbalance λ_0 is zero ($|\Delta k| = |\Delta k^\pm| = |k_e^\pm - k_h^\pm| = 0$) in each WP and the transport phase $\varphi_0 = 0$. There is no additional phase accumulation with the superconducting phase difference φ . In the first harmonic approximation, the total Josephson current is

$$\begin{aligned} J &= J_{H_F^+} + J_{H_F^-} \\ &= (J_+ + J_-) \sin \varphi. \end{aligned} \quad (12)$$

The CPR for FFLO-like pairing is shown in Fig. 3(c) and (d). Fig. 3(c) is the CPR for different L with fixed λ_0 and Fig. 3(d) is the CPR for different λ_0 with fixed L . The junction is always a 0 -junction.

The chiral anomaly induced $0-\pi$ transitions for BCS-like pairing is also verified by the evolution of ABSs by numerically solving Eq. (7). Fig. 4 shows the numerical

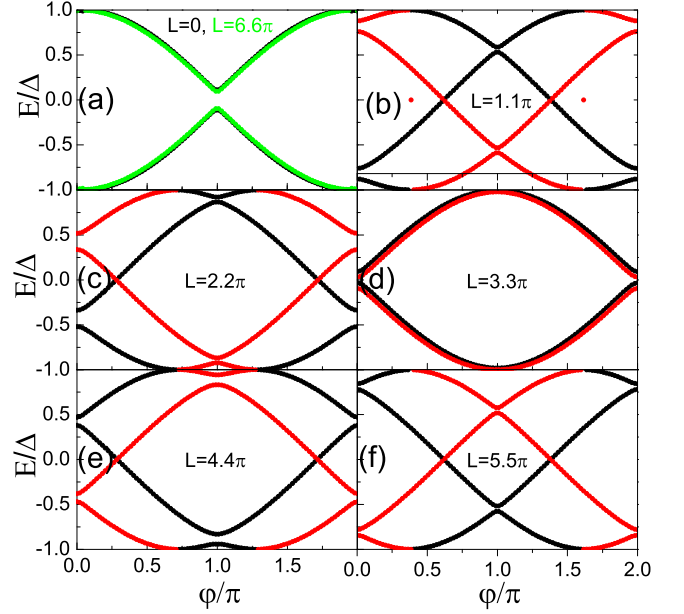


FIG. 4. Energy levels E_b of the Andreev bound states (solutions of Eq. (7)) for BCS-like pairing. In (b)-(f), the black curves represent bound levels for the pair H_B^+ and the red curves represent the bound levels for the pair H_B^- . The other parameters are the same as in Fig. 3(a).

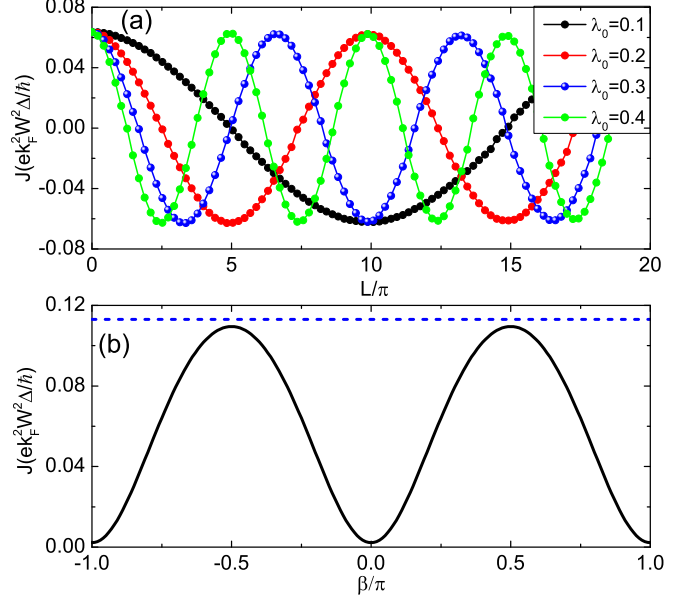


FIG. 5. (a) The Josephson current $J(\pi/2)$ for BCS-like pairing as a function of L for various λ_0 , the other parameters are the same as those in Fig. 3(a). (b) The Josephson current $J(\pi/2)$ as a function of the angle β , for BCS-like pairing (black solid line) and FFLO-like pairing (blue dotted line), the other parameters are $L = 0$, $\lambda_0 = 0.3$, $\mu = 0.3$ and $T = 0.5T_c$.

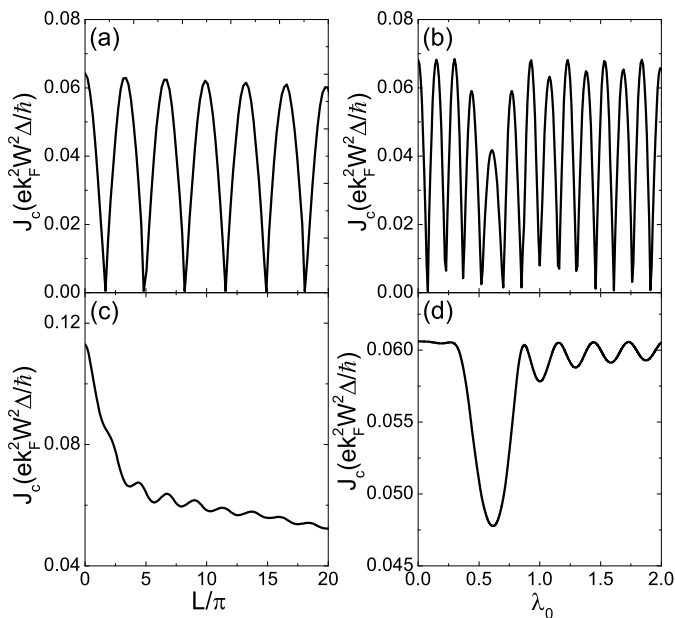


FIG. 6. (Left panel) The critical current J_c as a function of the length L with fixed $\lambda_0 = 0.3$ for BCS-like (a) and FFLO-like pairing (c). (Right panel) The critical current J_c as a function of λ_0 with fixed length $L = 6.6\pi$ for BCS-like (b) and FFLO-like pairing (d). The other parameters are $\beta = \pi/4$, $\mu = 0.3$ and $T = 0.5T_c$.

results of ABSs E_b with increasing L but fixed λ_0 . For $L = 0$, the ABSs for the two pairs H_B^\pm are degenerate as shown by the black dotted line in Fig. 4(a). For $L = 1.1\pi$, the ABSs for the pairs H_B^\pm split while the electron-hole symmetry $E \rightarrow -E$ is preserved. The ABSs of the two pairs become degenerate again at $L = 3.3\pi$ and the junction becomes a π -junction, as shown in Fig. 4(d). Further increase in the length L of the WSM splits the ABSs in opposite directions and the degeneracy of ABSs appears again at $L = 6.6\pi$. The junction becomes a 0-junction again as shown by the green dotted lines in Fig. 4(a). This periodic evolution of the ABSs with increasing L is an indubitable evidence of $0-\pi$ transitions induced by the chiral anomaly.

To verify the periodicity of the $0-\pi$ transitions, the Josephson current at $\varphi = \pi/2$ is plotted as a function of L for different values of the chirality imbalance λ_0 in Fig. 5(a). The periodic oscillations of the Josephson current are well fitted by Eq. (11). The junction is a 0-junction for $\lambda_0 L \approx 2n\pi$, but a π -junction for $\lambda_0 L \approx (2n+1)\pi$.

For the case of BCS-like pairing, the Josephson current also depends on the angle β between the line joining the two WPs and the transport direction due to the effective β -dependent superconducting gap $\Delta_B = \Delta_0 |\sin \beta|$. For $\beta = 0$ and $\pm\pi$, the WSCs have vanishing effective gap and the Josephson current would be minimum. For $\beta = \pm\pi/2$, the effective gap is maximum and the Josephson current would be maximum. The β -dependent Josephson current is shown by the black curve in Fig.

5(b). By contrast, the effective gap of the WSC for FFLO-like pairing is independent of β , and the corresponding Josephson current is also independent of β as shown by the blue dotted line in Fig. 5(b).

Furthermore, we consider the easily accessible experimental signal: the critical current J_c . Fig. 6(a) and (c) show the critical current as a function of the length L with fixed λ_0 for BCS- and FFLO-like pairing respectively. The dips in the critical current for BCS-like pairing (Fig. 6(a)) insure the $0-\pi$ transitions. By contrast, for FFLO-like pairing, J_c mainly decreases with increasing L (Fig. 6(c)), with small oscillations due to the normal multi-reflection at the interfaces. A similar behavior can be found in Fig. 6(b) where J_c is plotted as a function of λ_0 with fixed L . The constant period of the oscillations in J_c with increasing λ_0 is well consistent with $J_c = 2J_0 |\cos(\lambda_0 L)|$ as expressed in Eq. (11). Therefore, the chiral anomaly induced $0-\pi$ transitions should be easily observable in experiments by increasing λ_0 via increasing parallel \mathbf{E} or \mathbf{B} field. On the other hand, there is a big dip in J_c for FFLO-like pairing (Fig. 6(d)) which locates at $\lambda_0 \approx 2\mu$ where the chemical potential crosses the Weyl point. The successive small oscillations after the big dip are also from the transmission resonance due to the normal reflection. Therefore, this easily accessible experimental signal, J_c , can be used to distinguish the BCS-like pairing from the FFLO-like pairing in WSCs.

Finally, we comment on the experimental feasibility of the observation of chiral anomaly induced supercurrent oscillations in WSMs. The unconventional superconductivity observed in WoTe_2 ^{48,49} and Upt_3 ^{50,51} implies promising candidates for WSC. WSCs can also be achieved by the proximity effect of a conventional superconductor on a WSM. Because the model and conclusion in this work is quiet general, the predicted chiral anomaly induced $0-\pi$ transition may also be observable in such WSCs. Moreover, we suggest a thin film as the junction geometry for the WSC/WSM/WSM junction which is narrow in the y direction. The axis that connects two WPs is suggested to be laid along the x direction, because the Josephson current is maximum at $\beta = \pi/2$ for BCS-like pairing. An $\mathbf{E} \cdot \mathbf{B}$ field is also applied along the x axis to induce a chirality imbalance. In such a configuration, the side effects of the $\mathbf{E} \cdot \mathbf{B}$ field, such as the longitudinal voltage bias of the electric field, the orbital effect of the magnetic field, and the disturbance of the superconductivity can be well suppressed. The separate modulation of \mathbf{E} or \mathbf{B} field will tune the chirality imbalance λ_0 , and therefore lead to $0-\pi$ transitions and supercurrent oscillations in the case of BCS-like pairing.

IV. CONCLUSION

In conclusion, we numerically investigate the effect of chiral anomaly on the Josephson current in a WSC-WSM-WSC junction. We consider two types of pairing mechanisms: the BCS-like and FFLO-like pairings. For

BCS-like pairing, the chirality imbalance λ_0 induces a wave-vector difference between the electron and the hole in a Andreev bound state. This difference in wave-vector causes a transport phase which results in $0-\pi$ transitions in the CPR. The critical Josephson current oscillates as a cosine function of $\lambda_0 L$. Furthermore, the amplitude of the Josephson current depends on the angle β between the line joining the two WPs and the transport direction. However, for FFLO-like pairing, the junction always behaves as a 0 -junction and the Josephson current is independent of β . The experimental observation of this predicted chiral anomaly induced $0-\pi$ transition in the

Josephson current can verify the chiral anomaly effect and as well as distinguish the superconducting pairing mechanism of Weyl semimetals.

ACKNOWLEDGMENTS

The work described in this paper is supported by the National Natural Science Foundation of China (NSFC, Grant Nos. 11774144, and 11574045).

-
- * phjliu@gzhu.edu.cn
- ¹ M. Z. Hasan and C. L. Kane, Rev. Mod. Phys. **82**, 3045 (2010).
 - ² X.-L. Qi and S.-C. Zhang, Rev. Mod. Phys. **83**, 1057 (2011).
 - ³ X. Wan, A. M. Turner, A. Vishwanath, and S. Y. Savrasov, Phys. Rev. B **83**, 205101 (2011).
 - ⁴ S. Adler, Phys. Rev. **177**, 2426 (1969).
 - ⁵ P. E. C. Ashby and J. P. Carbotte, Phys. Rev. B **89**, 245121 (2014).
 - ⁶ P. Hosur, S. A. Parameswaran, and A. Vishwanath, Phys. Rev. Lett. **108**, 046602 (2012).
 - ⁷ W. Witczak-Krempa and Y. B. Kim, Phys. Rev. B **85**, 045124 (2012).
 - ⁸ O. Vafek and A. Vishwanath, Ann. Rev. Condens. Matter Phys. **5**, 83 (2014).
 - ⁹ M. M. Vazifeh and M. Franz, Phys. Rev. Lett. **111**, 027201 (2013).
 - ¹⁰ R. R. Biswas and S. Ryu, Phys. Rev. B **89**, 014205 (2014).
 - ¹¹ Y. Ominato and M. Koshino, Phys. Rev. B **89**, 054202 (2014).
 - ¹² B. Sbierski, G. Pohl, E. J. Bergholtz, and P. W. Brouwer, Phys. Rev. Lett. **113**, 026602 (2014).
 - ¹³ U. Khanna, A. Kundu, S. Pradhan, and S. Rao, Phys. Rev. B **90**, 195430 (2014).
 - ¹⁴ A. A. Burkov, J. Phys.: Condens. Matter **27**, 113201 (2015).
 - ¹⁵ D. T. Son and B. Z. Spivak, Phys. Rev. B **88**, 104412 (2013).
 - ¹⁶ A. A. Burkov, Phys. Rev. Lett. **113**, 247203 (2014).
 - ¹⁷ E. V. Gorbar, V. A. Miransky, and I. A. Shovkovy, Phys. Rev. B **89**, 085126 (2014).
 - ¹⁸ Qiang Li, Dmitri E. Kharzeev, Cheng Zhang, Yuan Huang, I. Pletikosić, A. V. Fedorov, R. D. Zhong, J. A. Schneeloch, G. D. Gu, and T. Valla, Nat. Phys. **12**, 550 (2016).
 - ¹⁹ K.-Y. Yang, Y.-M. Lu, and Y. Ran, Phys. Rev. B **84**, 075129 (2011).
 - ²⁰ A. A. Burkov and L. Balents, Phys. Rev. Lett. **107**, 127205 (2011).
 - ²¹ S. Murakami, New J. Phys. **9**, 356 (2007).
 - ²² A. M. Turner and A. Vishwanath, arXiv:1301.0330.
 - ²³ H. Weng, C. Fang, Z. Fang, B. A. Bernevig, and X. Dai, Phys. Rev. X **5**, 011029 (2015).
 - ²⁴ S.-M. Huang, S.-Y. Xu, I. Belopolski, C.-C. Lee, G. Chang, B. Wang, N. Alidoust, G. Bian, M. Neupane, C. Zhang, S. Jia, A. Bansil, H. Lin, and M. Z. Hasan, Nat. Commun. **6**, 7373 (2015).
 - ²⁵ S.-Y. Xu, I. Belopolski, N. Alidoust, M. Neupane, G. Bian, C. Zhang, R. Sankar, G. Chang, Z. Yuan, C.-C. Lee, S.-M. Huang, H. Zheng, J. Ma, D. S. Sanchez, B. Wang, A. Bansil, F. Chou, P. P. Shibayev, H. Lin, S. Jia, and M. Z. Hasan, Science **349**, 613 (2015).
 - ²⁶ B. Q. Lv, H. M. Weng, B. B. Fu, X. P. Wang, H. Miao, J. Ma, P. Richard, X. C. Huang, L. X. Zhao, G. F. Chen, Z. Fang, X. Dai, T. Qian, and H. Ding, Phys. Rev. X **5**, 031013 (2015).
 - ²⁷ S.-Y. Xu, N. Alidoust, I. Belopolski, Z. Yuan, G. Bian, T.-R. Chang, H. Zheng, V. N. Strocov, D. S. Sanchez, G. Chang, C. Zhang, D. Mou, Y. Wu, L. Huang, C.-C. Lee, S.-M. Huang, B. Wang, A. Bansil, H.-T. Jeng, T. Neupert, A. Kaminski, H. Lin, S. Jia, and M. Z. Hasan, Nat. Phys. **11**, 748 (2015).
 - ²⁸ S.-Y. Xu, I. Belopolski, D. S. Sanchez, C. Zhang, G. Chang, C. Guo, G. Bian, Z. Yuan, H. Lu, T.-R. Chang, P. P. Shibayev, M. L. Prokopovych, N. Alidoust, H. Zheng, C.-C. Lee, S. M. Huang, R. Sankar, F. Chou, C.-H. Hsu, H.-T. Jeng, A. Bansil, T. Neupert, V. N. Strocov, H. Lin, S. Jia, and M. Z. Hasan, Sci. Adv. **1**, e1501092 (2015).
 - ²⁹ Z. Wang, Y. Zheng, Z. Shen, Y. Zhou, X. Yang, Y. Li, C. Feng, and Z.-A. Xu, Phys. Rev. B **93**, 121112 (2016).
 - ³⁰ G. Xu, H. Weng, Z. Wang, X. Dai, and Z. Fang, Phys. Rev. Lett. **107**, 186806 (2011).
 - ³¹ J. Y. Liu *et al.*, Nat. Mater. **16**, 905 (2017).
 - ³² Qiunan Xu, Enke Liu, Wujun Shi, Lukas Muechler, Jacob Gayles, Claudia Felser, and Yan Sun, Phys. Rev. B **97**, 235416 (2018).
 - ³³ C. Fang, M. J. Gilbert, X. Dai, and B. A. Bernevig, Phys. Rev. Lett. **108**, 266802 (2012).
 - ³⁴ G. Y. Cho, J. H. Bardarson, Y.-M. Lu, and J. E. Moore, Phys. Rev. B **86**, 214514 (2012).
 - ³⁵ P. Fulde and R. A. Ferrell, Phys. Rev. **135**, A550 (1964).
 - ³⁶ T. Zhou, Y. Gao, and Z. D. Wang, Phys. Rev. B **93**, 094517 (2016).
 - ³⁷ H. Wei, S.-P. Chao, and V. Aji, Phys. Rev. B **89**, 014506 (2014).
 - ³⁸ G. Bednik, A. A. Zyuzin, and A. A. Burkov, Phys. Rev. B **92**, 035153 (2015).
 - ³⁹ W. Chen, L. Jiang, R. Shen, L. Sheng, B. G. Wang, and D. Y. Xing, Europhys. Lett. **103**, 27006 (2013).
 - ⁴⁰ S. Uchida, T. Habe, and Y. Asano, J. Phys. Soc. Jpn. **83**, 064711 (2014).

- ⁴¹ K. A. Madsen, E. J. Bergholtz, and P. W. Brouwer, Phys. Rev. B **95**, 064511 (2017).
- ⁴² U. Khanna, D. K. Mukherjee, A. Kundu, and S. Rao, Phys. Rev. B **93**, 121409 (R) (2016).
- ⁴³ U. Khanna, S. Rao, and A. Kundu, Phys. Rev. B **95**, 201115(R) (2017).
- ⁴⁴ D. K. Mukherjee, S. Rao, and A. Kundu, Phys. Rev. B **96**, 161408(R)(2017).
- ⁴⁵ Y. Xu, S. Uddin, J. Wang, Z. Ma, and J.-F. Liu, Phys. Rev. B **97**, 035427 (2018).
- ⁴⁶ Jun Fang, Wenye Duan, Junfeng Liu, Chao Zhang, and Zhongshui Ma, Phys. Rev. B **97**, 165301 (2018).
- ⁴⁷ J.-F. Liu and K. S. Chan, Phys. Rev. B **82**, 184533 (2010).
- ⁴⁸ Y. Sun, S.-C. Wu, M. N. Ali, C. Felser, and B. Yan, Phys. Rev. B **92**, 161107 (2015).
- ⁴⁹ Y. Qi, P. G. Naumov, M. N. Ali, C. R. Rajamathi, O. Barkalov, M. Hanfland, S.-C. Wu, C. Shekhar, Y. Sun, V. Süb, M. Schmidt, E. Pippel, P. Werner, R. Hillebrand, T. Förster, E. Kampertt, W. Schnelle, S. Parkin, R. J. Cava, C. Felser, B. Yan, and S. A. Medvedev, Nat. Commun. **7**, 11038 (2016).
- ⁵⁰ R. Joynt and L. Taillefer, Rev. Mod. Phys. **74**, 235 (2002).
- ⁵¹ Y. Yanase, Phys. Rev. B **94**, 174502 (2016).